Journal citation: Computational and Theoretical Polymer Science, 2001, 11, *175-189.*

The Conformational Structures of Defect-Containing Chains in the Crystalline Regions of Isotactic Polypropylene*

Marc R. Nyden
Building and Fire Research Laboratory
National Institute of Standards and Technology
Gaithersburg, MD 20899
mnyden@nist.gov

D.L. Vanderhart
Polymers Division
National Institute of Standards and Technology
Gaithersburg, MD 20899

Rufina G. Alamo
Department of Chemical Engineering
Florida Agricultural Mechanical University-Florida State University
2525 Pottsdamer Street
Tallahassee, FL 32310-6046

Abstract

Calculations were performed to assign defect-resonance patterns observed in solid state ^{13}C NMR spectra obtained from the crystalline regions of isotactic polypropylene. The spectral features of interest are associated with stereo, regio, and comonomer-type defects which can typically be found in metallocene-synthesized polymers. The calculations were carried out as follows: A model of the crystalline region of defect-free isotactic polypropylene was constructed from available X-ray data corresponding to the α-lattice. A series of irregularities including ethylene comonomer, stereo-mrrm, regio 2,1-erythro, and butylene comonomer defects were introduced one at a time at various positions in a specific stem occupying a central position in the model crystallite. Low-lying conformations were then obtained from simulated annealing calculations that were initiated from these structures. Finally, quantum mechanical calculations were performed on representative segments of the defect-containing chains excised from the annealed crystallites and the calculated chemical shifts were compared to the observed resonances. The results of the calculations were used as a basis for interpreting the NMR intensities of defect-related resonances in terms of the partitioning of defects and to help establish the conformational structures of the defect-containing stems.

Keywords: Isotactic, Polypropylene, C13, NMR, Solid state, Defects, Stereo, Regio, Partioning, Assignments, Simulated annealing, Quantum mechanical calculations

Introduction

There is widespread commercial interest in designing polymers to possess specific properties. Metallocene catalyzed isotactic polypropylenes (iPP's) offer great promise in this regard because of the wide variety of structures that can be obtained by controlling irregularities (or 'defects'), introduced during their synthesis. It is known that these irregularities, which commonly include stereo, regio and comonomer-type defects, can have a significant effect on both mechanical and process related properties [1]. This is especially true if defects are fully rejected from the crystalline (CR) regions. For the 4 defect types considered in this paper, the situation is more complicated in that each defect has been shown [2,3,4], by solid-state NMR, to be discriminated against, but not fully rejected in the crystallization process. A thorough understanding of the relationship between the nature of defects, their conformation and conformational structure in a CR lattice, and their partitioning values has yet to emerge. In this paper we undertake computations which a) look for minimum-energy conformations for these defects in the CR lattice of iPP and b) predict, via *ab initio* calculations, the isolated-molecule chemical shifts for carbons at or near these defect sites in these energy-minimized conformations. Full success in this endeavor would enable us a) to interpret correctly the NMR spectral intensities of the CR regions of these iPP's in terms of the concentration of defects, b) establish, via the agreement of calculated and observed chemical shifts, the conformations of the CR stems that contain the defects and c) to appreciate the role of defect energies in determining the partitioning of defects between the CR and noncrystalline (NC) regions. With the results reported in this paper, we believe that we have made substantial progress towards the achievement of the first two of these objectives. However, additional work will be required before we are able to provide a clear picture of the energetic considerations that govern whether a specific type of defect will be accepted or rejected from the CR.

The structures with which we deal in this paper include the following:

1) The *defect-free iPP chain* can be represented as:

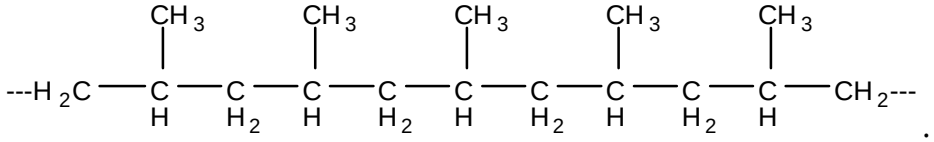

2) The *ethylene-comonomer defect* involves a substitution of an ethylene for a propylene molecule in the polymerization:

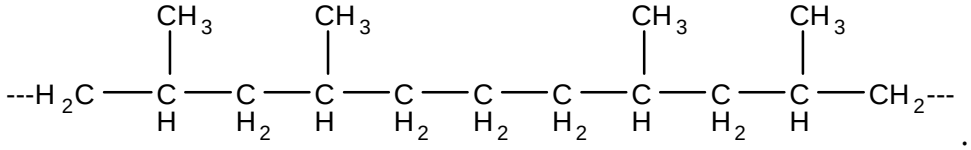

3) A *stereo-mrrm defect* involves the preservation of head-tail polymerization but an exchange of the positions of the hydrogen and the methyl group on a single isolated methine carbon:

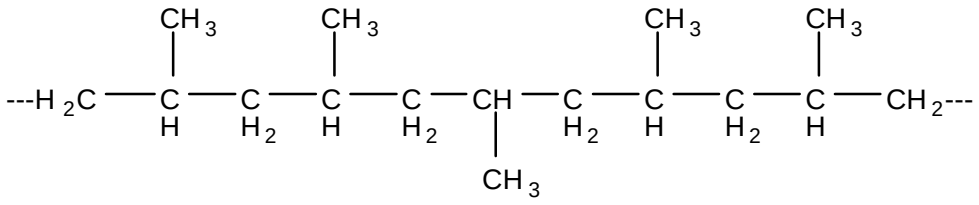

4) A *regio 2,1-erythro defect* is a type of head-head (and tail-tail) defect where the methyl groups have a particular stereopositioning:

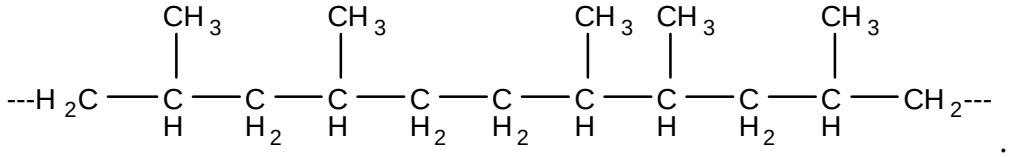

5) The isolated *butylene-comonomer defect* is given as follows, where we assume that the ethyl branch occupies only the normal stereochemical position that the methyl group would have occupied:

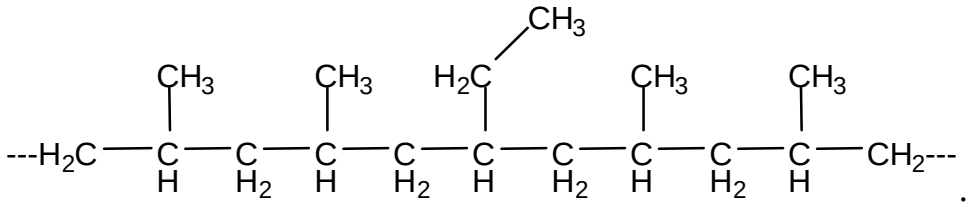

The extent to which polymer chains containing these defects are incorporated into crystalline regions of iPP was examined in previous solid-state NMR studies where estimates for the crystalline partition coefficients,

$$P_{CR}(def) = \frac{C_{CR}(def)}{C_{Ave}(def)}, \tag{1}$$

are reported [2,3,4]. In this equation, C_{CR}(def) denotes the concentration of a given defect in the CR region and C_{Ave}(def) is the sample-average concentration. These quantities are determined, respectively, from solid-state and solution-state NMR.

The accuracy of NMR chemical shifts calculated at various levels of theory was investigated in a recent paper by Cheeseman, *et al* [5]. Quantum mechanical calculations, based on both the Hartree Fock (HF) and a series of density functional (DFT) methods, using two different approaches to gauge invariance (GIAO and CSGT) as a function of basis set, were performed on a set of 20 small molecules. These investigators concluded that accurate estimates of ^{13}C chemical shifts (the RMS error was 4.2 ppm) for small molecules can be obtained from GIAO calculations (which makes use of explicit magnetic-field-dependent basis functions) at the B3LYP/6-311+G(2d,p) level of theory. In fact, in the application we discuss, only the *differences*

between the chemical shifts for the polymer of interest and those of a reference polymer are needed for most of the carbons and, as will be seen, these differences applied to the experimental shifts for the defect-free CR polymer predict the chemical shifts of the carbons near a defect with more precision than is available from the direct calculation of chemical shifts.

Chemical shifts are quite sensitive to conformational structure [6]. This is advantageous because it implies that agreement between the calculated and experimental chemical shifts for a given conformation is strong evidence in support for that conformational structure. However, the detailed conformation for defects like the regio 2,1 erythro defect or the stereo-mrrm defect depend on how well we can model the lattice. In fact, if one were to preserve the 3_1 helix for the backbone carbons of defect-free iPP [20], these 2 defects would yield unacceptably high energies. Hence, given the constraints of the surrounding molecules and given the need to move away from the helical structure while maintaining the overall linearity of the molecule, one would expect that the minimum-energy conformations would depart substantially from the usual trans and gauche dihedral angles. The foregoing considerations prepare us for some uncertainty in both the chemical shift calculations and in the conformations obtained from energy-minimization calculations. Despite these uncertainties, we will be able to identify, for each of the defect types considered in this study, at least one low-lying conformation for which the relative chemical shifts are in reasonable agreement with the experimental values.

The minimum-energy conformations were determined from a series of calculations that we now describe. First, the defects were introduced at various sites in a molecular model of the α form [8] of crystalline iPP. Low lying conformers were then obtained by simulated annealing. Finally, the chemical shifts of carbons in the defect-containing chains were evaluated by performing quantum mechanical calculations on representative segments excised from the annealed crystallites.

Procedures

Experimental. The solid state ^{13}C NMR spectra were acquired at 2.35 T (25.2 MHz) on a non-commercial spectrometer. Spectra were taken at ambient temperature using a magic angle spinning (MAS) frequency of 4.0 kHz and nutation frequencies, associated with the strengths of the ^{13}C and proton radiofrequency fields, of 66 kHz and 62 kHz, respectively. The typical period between acquisitions was 4 s and the usual signal observation window, with high-power proton decoupling, was 140 ms. Separation of the ^{13}C signals [7] arising from the crystalline and non-crystalline regions of iPP was based on differences in the intrinsic rotating-frame relaxation times, $T_{1\rho}{}^{H}$, as well as linewidth differences associated with each region. Very long acquisition times, in some cases 10 to 12 days corresponding to about 100,000 scans, were needed to obtain CR spectra with sufficiently good signal-to-noise to discern defect intensities on the order of 10^{-3} times each parent resonance. Finally, the 'defect' spectra that we will consider are presented to illustrate only one thing, namely, *the correct positions and relative intensities of the defect-related resonances.* In other words, relative intensities of the main iPP backbone resonances have no direct meaning because these spectra have been 'corrected' for the presence of other types of defects. It was impossible for us to find samples that had sufficient amounts of a given defect but also had no contamination from other defects. Hence, starting with the CR spectrum of a sample whose dominant defect was the defect of interest, we corrected for the minor, interfering defects by subtracting appropriately-scaled CR spectra associated with samples dominated by the interfering defects. The assumption made in scaling these subtracted spectra

was that the level of each defect in the CR region is directly proportional to the overall concentration of that defect, which is known from solution-phase NMR measurements [2], and is independent of the presence of other types of defects in the lattice. A more detailed description of the preparation and characterization of the samples and the technique used to discriminate between signals arising from the CR and NC regions of the polymer may be found elsewhere [2,3,7].

Computational. A molecular model of the α crystallite of iPP was constructed by applying the appropriate C2/c symmetry transformations to the fractional coordinates for the asymmetric unit as reported in reference [8]. A similar model was used previously by Rutledge and Suter in their molecular mechanics study of relaxation mechanisms in iPP [9]. Hydrogens were added such that the initial C-H bond distances and H-C-H bond angles were 0.109 nm and 109.5°, respectively. These values, however, were allowed to (and did) change during the simulated annealing procedure which is described in subsequent paragraphs. The model crystallite used in all of the calculations consisted of 26 stems each containing 21 repeat units arranged in a 3_1 helix characterized by an alternating sequence of trans and gauche dihedral angles. This structure is depicted in the form of a projection in the plane normal to the C axis in Figure 1. Notice that the 3_1 helices appear as equilateral triangles with the methine and methylene carbons nearly superimposed at the vertices and the methyl carbons extending outward from these vertices. Backbone bonds in this helix can easily be seen to alternate between strong projections parallel and perpendicular to the chain axis.

Defects were introduced, one at a time, in one of the two central chains (indicated by the arrow) depicted in Figure 1. Because the symmetry of the lattice is not that of the 3_1 helix, the 3 consecutive positions for the defect over 1 turn of the helix need not have identical intermolecular potentials. For this reason, we might expect the minimum-energy conformation to be a weak function of lattice position. Therefore, at least three initial structures were investigated for each defect type, corresponding to the 3 consecutive placements of the defect around 1 turn of the 3_1 helix. In all cases, the defects were positioned so that they were approximately in the center of the stem. This was done to ensure that the calculations were representative of defects in the interior of the CR, rather than near the CR/NC interface.

The simulated annealing calculations, which consisted of heating the model crystallite to a constant temperature of 600 K for 100 MD time steps and then relaxing (cooling) it by performing 100 iterations of the Polak Ribiere conjugate gradient minimization, were performed using Discover_95[**] with the Consistent Valence Forcefield (CVFF) [10]. The nonbond potential energy interactions were evaluated using the cell multipole summation [11] option with default values for the number of neighboring cells (26) and order of the highest multipole (2) parameters. The validity of this approach was evaluated by performing calculations that were otherwise identical except that the nonbond potential energy terms were explicitly calculated up to a cut-off distance of 15×10^{-10} m between charge groups. The conformations obtained from both sets of calculations were nearly identical. In all cases, only the atoms in central chains and their first nearest neighbors (a total of 1910 atoms in 10 chains) were allowed to move. All of the atoms comprising the outer shell consisting of 16 (second nearest neighbor) chains was fixed to the same coordinates for the entire annealing simulation in an effort to preserve the overall structure of the crystallite. The heating and cooling cycle described above was repeated 50 times

[**] Certain commercial equipment, instruments, materials or companies are identified in this paper in order to adequately specify the experimental procedure. This in no way implies endorsement or recommendation by NIST.

for each initial placement of the defect. At the conclusion of this sequence, a minimum energy structure was obtained by iterating the conjugate gradient algorithm until the maximum derivative of the energy with respect to any degree of freedom was less than 42 J/nm. This typically required on the order of a few thousand iterations. These simulated annealing calculations were performed on model crystallites both with, and without, defects. The chemical shifts of the carbons from the defect-free chain in the lattice were used as references in correcting the values calculated for the carbons in the defect-containing chains *(vida infra)*.

Quantum mechanical calculations, in which the second derivatives of the energy with respect to the magnetic moment and magnetic field strength were evaluated for each carbon, were then performed on methyl-terminated oligomeric segments of the defective chains containing at least 7.5 repeat units. The isotropic chemical shifts were estimated as the average of the principal values of the second derivative tensor. These estimates were corrected for systematic errors by application of either Eq.(2) or Eq.(3) (see the discussion in the following section) and the resulting values were compared to the experimental defect-resonance pattern.

The chain segments used in the quantum mechanical calculations were excised from the annealed crystallite in such a way that the site of the defect was positioned near the center with an approximately equal number of backbone carbons on either side. In some cases, we also performed calculations on polymer segments containing two chains to investigate the possibility that the chemical shifts might be affected by interactions between neighboring chains. The segments used in these calculations consisted of two nearest-neighbor chains, one with 5.5 monomers (including the defect) and the other 3.5 monomers.

The quantum mechanical calculations were performed at the BLYP 6-311+G(2d,p) level of theory with Gaussian 98 [12] running on 8 processors (using 2 Gb of memory) of a 32 processor (300 Mhz R12000) SGI Origin 2000 workstation. The BLYP method, which is a pure DFT approach consisting of the Becke exchange [13] and Lee, Yang, Parr correlation functionals [14], requires less computer time than the corresponding calculations using the hybrid B3LYP method which was recommended in the paper by Cheeseman, *et. al* [5]. This was an important consideration because we had to use large fragments, sometimes containing as many as 9 repeat units, to account for gamma interactions on all of the affected carbons and we were already straining the available resources with the computationally less demanding BLYP calculations (typical run times were about 10 CPU hours). Our benchmark calculations on smaller fragments indicated that the accuracy of BLYP chemical shifts is comparable, at least in the case of polypropylene, to what would be obtained from the corresponding B3LYP calculations.

Errors

The calculated chemical shifts were corrected (to give the values denoted by CS_d) by application of Eq.(2) in an effort to remove systematic errors in the quantum mechanical calculations due to deficiencies in the description of electron correlation, the one-electron basis set, and the interactions between the electrons and the external magnetic field.

$$CS_d = CS_r^e + (CS_d^c - CS_r^c) \tag{2}$$

In this equation, CS^e_r and CS^c_r are the experimentally determined and computed chemical shifts for the specific type of carbon (*i.e.*, CH, CH_2, or CH_3) in the defect-free iPP oligomer and C^c_d is the computed value of the chemical shift obtained for defect-containing chain. The use of this

formula is based on the idea that the change in the chemical shift as a result of incorporation of the defect can be calculated to better accuracy than the absolute value because of a cancellation of errors. However, we have found that the magnitude of this error depends on whether the carbon in question is methine, methyl, or methylene (*vide-infra*). Thus, the application of this formula presumes some knowledge of the chemical nature of the carbons in the defect-containing chain so that the correct reference values can be employed. This creates an ambiguity when, in comparing the defective and the defect-free chains, there is any *change* in the type of carbon. This is the case for at least 1 carbon for all of the defect-containing chains except the stereo-mrrm defect. For carbons that change their type at the defect site, we used the linear correlation method, summarized in Eq.(3), to correct the chemical shifts of the atoms directly involved in the structural irregularity.

$$CS_d = aCS_d^c + b \tag{3}$$

The justification for using this formula to correct the chemical shifts is based on the linearity between the experimental and computed shifts which has been noted in previous studies conducted by other investigators [15-18]. The extent to which this linear relationship is obeyed in the polymers of interest is illustrated in Figure 2, which summarizes the computed and experimental chemical shifts for the carbons in iPP, iPP/ETH and the stereo-mrrm defect (but not the regio 2,1-erythro or iPP/BUT defects). Notice that the scatter about the linear regression line is systematic; with the chemical shifts of the methylene carbons being under-estimated and the methine carbons over-estimated. This implies that we can do better by employing a different correlation for each atom type, as in Eq.(2). Accordingly, we only used Eq.(3) when there was a change in the chemical nature of the atom as a result of the defect.

The major source of the residual error in the calculations, after applying the correction formulas discussed above, was determined to be the arbitrary variations in the bond and dihedral angles introduced during the simulated annealing calculations (*vide-infra)*. The resulting uncertainties in the calculated chemical shifts were, therefore, estimated as the standard errors of the values obtained from three independent realizations of the annealed conformer for each defect type. These random variations of the conformational structures of the annealed polymer were generated by initiating the simulated annealing calculations from structures where the defects were placed in different positions in the same chain. The determinations that the resulting structures were, in fact, different realizations of the same conformer (as opposed to being entirely different conformers) were made on the basis of agreement between the chemical shifts and energetics (*i.e.*, the quantum mechanical energies of the excised oligomers) and a detailed, semiquantitative, comparison of the dihedral angles.

Ideally, one would like to evaluate the energy costs associated with the accommodation of the various defect types in the crystal lattice. While the quantum mechanical energies of the excised oligomers give accurate and very precise energies, they do not account for the intermolecular contributions, which renders these calculations inadequate for the stated purpose. Therefore, we looked to the molecular mechanical energies, which are computed as part of the simulated annealing calculations, for supporting evidence that one conformer was preferred over another. Unfortunately, we found that the inclusion of the defects caused relatively modest perturbations in the energies that were of the same order as the rms variation in the lattice energies for the defect-free iPP. We attribute this lack of precision in the lattice energies (obtained from the molecular mechanics) to the accumulation of errors in the nonbonded

interactions (which although they may be individually small, are summed over the entire lattice) and to our inability to distinguish between the energetic consequences of the disorder resulting from accommodation of the defects and those due to random variations in the atomic positions at the end of the simulated annealing calculations (*vide supra*). We do note, however, that despite the fact that we are unable to make definitive statements about the relative energies (enthalpies) of the annealed crystals, all of the structures that we propose in subsequent sections of this paper for the defect-containing stems correspond to local energy minima that were stable to the annealing process. By this we mean that, once they were generated (which was usually in the first few annealing cycles), these conformations persisted until the conclusion of the annealing process (50 cycles). On the other hand, we also observed the formation of more transient structures, which in some cases actually had lower energies than the stable conformations referred to above, but were unstable to annealing in the sense that they would quickly convert to another structure after only a few annealing cycles. We note in passing, that although this persistence could, in principle, be indicative of a high entropy content (in that it implies that the system spends more time in this configuration), we cannot offer any quantitative evidence in support of this explanation. Thus, we are left defending the position that while we, on the one hand, admit the inability of these calculations to give us meaningful estimates of changes in lattice energy associated with certain defects, we still claim that these calculations do a reasonable job of finding the local minimum-energy conformations *in the vicinity of the defects*. In this regard, it should be stated that while we have a high degree of confidence in the ability of the force field to account for the intramolecular forces, we are very skeptical of its ability to account for the details of the interactions between stems. The justification for our position derives from the intuition that beyond the prerequisite of providing a crude representation of the excluded volume (associated with the nonbonded repulsions due to the other stems in the lattice), which (albeit necessary) almost any force field would be expected to furnish, it is the intramolecular forces that determine the conformational geometries of the minimum energy structures.

Results and Discussion

iPP

Calculations were performed on a model of the crystalline region of defect-free iPP to obtain reference values for the corrected chemical shifts that are reported in the following sections of this paper. The iPP segments were excised from the annealed crystallite such that each of the three unique methine carbons in the 3_1 helix occupied the central position of a chain. The mean values, obtained from calculations corresponding to each of these three locations, are reported for the carbon atoms in chains containing 7.5 and 8.5 repeat units along with the experimental chemical shifts in Table I. The uncertainties in the computed values were estimated from the corresponding standard errors. Although the absolute differences between the calculated and experimental chemical shifts are substantial, particularly for the methine carbons, the variation within any one of the three sets of chemically equivalent carbons (methines, methylenes, and methyls) is only on the order of a few tenths of a ppm. We attribute the deviations from the mean to random variations in the structure of the chains which are introduced during the simulated annealing calculations. In fact, we have noticed that, after annealing, dihedral angles can vary by as much as 10° (from the idealized values of -60° and 180°) in the same chain. Since these variations are random in nature, the resulting errors are not

eliminated, and may even be compounded by subtracting these reference values from the chemical shifts obtained for the defect-containing chains in the process of computing the corrected chemical shifts.

The exceptionally large disparity between the values obtained for the last methylene reported for the 7.5 and 8.5 monomer segments, however, is evidence of a difference that results from shortening the chain from 8.5 to 7.5 repeat units. The methine carbon on the outermost repeat unit of the longer chain provides a γ-gauche interaction [19] with this methylene carbon; in the shorter chain, this interaction is absent. Hence, consistent with the magnitude of γ-gauche effects on chemical shifts, the shift of this methylene is about 4 ppm upfield for the longer oligomer, relative to the shift of the shorter oligomer. Given this potential source of shift disparity, it seems prudent to eliminate this problem by using fragments that are large enough to account for all of the γ-gauche interactions for all carbons influenced by the defect.

Ethylene Comonomer Defect

This is the easiest defect to treat since the deviations in conformation of the backbone atoms are expected to be small. The set of calculated chemical shifts will also be seen to be in the best agreement with experimental shifts.

Chemical shift calculations for this defect have already been reported [3], where it was assumed that the backbone remains in the 3_1 helix described by the X-ray determined [20] atomic coordinates for the α-form of CR iPP. What we describe below are parallel results, using a simulated annealing approach to determining the conformation of both the defective and defect-free chains. This new approach, gratifyingly, leads to very similar predictions for the shifts.

The simulated annealing calculations on this defect were initiated from three independent structures generated by removing a methyl group from each of three unique methine carbons in a specific stem in the model crystallite as described in the previous section. In each case, the introduction of the defect had no effect on the equilibrated backbone conformation as evidenced by the fact that the annealed chains adopted the same conformation (3_1 helix) that was obtained when there were no defects. This is not surprising, since the substitution of a hydrogen atom for a methyl group would be expected to create more room for the defect-containing chain in the crystal. The conformational structure (obtained from one of the simulated annealing calculations, but representative of all three) is displayed in Figure 3.

The average value of the three sets of chemical shifts obtained from the annealed ethylene copolymer fragment are presented in Table II. The 12 values correspond to carbons in the vicinity of the defect. In referring to these carbons we adopt a numbering system in which the order is methylene, methyl, methine, where numbering begins and ends with a methylene. This convention is used throughout the rest of this paper. Note, however, that there are some issues that arise in reference to specific defects. Thus, for example, in the case of iPP/ETH, carbon 5 corresponds to the methyl carbon that was removed to create the comonomer defect. In general, we found that, for all of the defect types considered in this study, chemical shift changes, with respect to the reference chain, were insignificant outside of this region. The numbered region consists of about 4.5 monomers including the site of the defect. In the case of the ethylene comonomer defect, only 4 of the 12 carbons in this region actually had chemical shifts that deviated from the reference by more than the estimated uncertainty in the calculations.

The corrected chemical shifts, which were obtained via Equation 2, are in good agreement with the shifts of the observed, weaker defect-related resonances. In Figure 4, a

vertically amplified spectrum of the crystalline regions of an iPP/ethylene copolymer with a mole fraction of 0.075 ethylene is shown. One can clearly see the weaker resonances, associated with the defect, that lie between the main methine (26.7 ppm) and the methylene (44.5 ppm) resonances. Arrows indicate the positions of the calculated chemical shifts. The good agreement between calculations and experiment supports the hypothesis that the copolymer is incorporated in the crystallite with the same chain conformation (3_1 helix) as the homopolymer. The apparent accuracy of these calculated chemical shifts presumably reflects a cancellation, via this difference method, of the computational errors due to compromises in the level of theory. As noted above, the errors in the absolute shifts are much more significant ranging from a few tenths of a ppm in the methyl carbons to almost 8 ppm in the methine carbons.

The assignments based on the calculations (Table II) reveal that there are significant shifts, relative to the homopolymer, for the sequence of three consecutive methylene carbons (C4, C6 and C7) and one of the two methine carbons (C3). The chemical shift of the other proximate methine (C9) is almost unaffected by the transformation from homopolymer to copolymer. A rationalization of the calculated shift differences in terms of recognized effects has been given [3], and we reiterate the essential points as follows: The C5 methyl carbon, that becomes a hydrogen in the generation of the ethylene defect, was originally γ-gauche to the C3 methine carbon and trans to C9. Hence, for the defective chain, the shift of C3 will move downfield by about 4 ppm to 6 ppm [19], relative to the shift of C9, because a γ-gauche interaction is lost only at C3. This loss also results in a similar change in chemical shift for the interior carbons, C4 and C6, that defined the carbon sequence of the lost gauche dihedral angle; these carbons lose a “vicinal gauche” interaction [21]. Thus, C4 is expected to experience a shift change of about 2.7 ppm compared to the shift of C7. These arguments account for the major portion of the observed and calculated shift differences between methine carbons C3 and C9 and between methylene carbons C4 and C7. Based on the foregoing, the observed defect resonances at 31.1 ppm (C3), 34.7 ppm (C7), and 39.2 ppm (C4) each arise from a single carbon on the defect-containing chain. This is consistent with the relative intensities obtained by integration of the peaks in the experimental spectrum and results in the value, $P_{CR} = 0.42 \pm 0.03$, for the crystalline partition coefficient of this defect [3].

The methine carbon (C6) in the defect-free iPP that was converted to a methylene carbon in the defective oligomer, is a carbon whose shift cannot be predicted by Equation 2 since it changed type; thus, Equation 3 must be used, based on the fit shown in Figure 2. One can see a hint of the experimental resonance position in Figure 4 between the methyl and methine resonances. This experimental shift of 24.5 ppm was confirmed using polarization/depolarization experiments [3]. Table 2 indicates that the disparity between calculated and experimental shifts is quite large (1.6 ppm) for this carbon. This is not unexpected since we recognize Equation 3 to give poorer estimates of the shift values.

It is of interest to note, that the corrected chemical shifts reported in reference [3], which were computed from the differences in the chemical shifts obtained before and after the deletion of a methyl group from the X-ray determined structure (i.e., without simulated annealing), are in better agreement with experiment than are the values reported in Table II. Thus, it appears that the assumption that the conformational structure is unaffected by the introduction of this defect actually introduces less error than the simulated annealing calculations (*vida supra*). This reinforces our suspicion that a significant source of the residual error in the computed shifts using Equation 2 is introduced by minor variations in the minimum-energy conformations. At the same time, we continue to believe that using an energy-minimized reference chain is the correct

procedure. It seems right that both the defect-free and the defective chains should be minimized using the same force fields in order to avoid the criticism that the crystal structure may not represent a minimum-energy conformation for the force field used.

Unfortunately, the convenient assumption that the ethylene defect is incorporated without a change in the iPP backbone conformation cannot be expected to apply to the stereo- and regio-type defects considered below. For these defects, the displacement, rather than elimination, of a methyl group leads to unacceptably high energies when the helical conformation of the backbone is preserved; hence, significant departures, not only from the usual backbone conformation, but also from the usual trans and gauche dihedral angles are expected. When that happens, we no longer can invoke, with confidence, the more qualitative arguments about γ-gauche or vicinal-gauche effects in order to interpret the observed chemical shifts; rather we will have to depend heavily on the shift calculations associated with each energy-minimized conformation.

Stereo-mrrm Defect

The calculations relating to this defect were initiated from structures obtained by interchanging the coordinates of the hydrogen atom and methyl group on each of the 3 unique methines carbons in the 3_1 helix of iPP. There were only minor variations in the dihedral angles, lattice energies, and the calculated chemical shifts for each initial placement of the defect. The average chemical shifts, which were computed as the mean values obtained from these three independent calculations, are presented in Table III. The extent of the agreement between the calculated and observed resonances is indicated in Figure 6 which shows a difference spectrum (see Figure caption) emphasizing the resonances associated with the stereo-mrrm defect. The arrows are used to indicate the positions of the chemical shifts obtained from the calculations after they were corrected by the application of Eq.(2). This is the only defect that we treat where there is a full correspondence of carbons with those of the reference chain so that there is no need to invoke Eq. 3.

The conformation corresponding to these chemical shifts is displayed in Figure 5. It is essentially helical except for a departure, in the immediate vicinity of the defect, from the alternating backbone sequence of trans and gauche dihedral angles that characterizes the 3_1 helix. This deviation consists of a series of 3 consecutive (approximately) trans dihedral angle followed by one gauche angle with the opposite sign (i.e., $60° \pm 5°$ rather than $-60° \pm 5°$) along the backbone of the chain. In addition, the value of one of the dihedral angles, which was trans in iPP, is only about 140° in the stem containing the stereo mrrm defect. Changing the sign of the gauche dihedral angle involves major movement of the atoms and we found that we had to go to higher temperatures (800 K) in the annealing simulations to generate this conformation. In this regard, it is important to note that, although this temperature is inordinately high, the total simulation time (50×10^{-12} s) was extremely short. Thus, our simulations essentially represent brief fluctuations in the annealing process that allow a crossing of high-energy barriers in the process of exploring conformational space. In this context, it is also significant to note that, despite the high temperatures used in these simulations, the excursions in molecular structure were never severe enough to cause the translation or translation/rotation of stem resulting in a change in the elevation of carbons to a new lattice position.

In trying to understand why this conformation is adopted by the defect-containing chain, it is in important to recall that in the 3_1 helix, which is the preferred conformation for iPP, each methyl experiences only one γ-gauche interaction (with a methine carbon). Meanwhile, methine

carbons each normally experience 2 γ-gauche interactions, one with a methyl in one direction and the other with a methylene in the other direction. Thus, using Figure 3 as an example, each methyl is normally gauche with respect to the first methine on the left, but trans with respect to the first methine on the right. However, when the coordinates of the hydrogen and the methyl (C5) bonded to C6 are interchanged in the process of creating the stereo defect (assuming for the moment that the structure of the 3_1 helix is preserved), the first γ-gauche interaction between C5 and C3 is preserved while a second γ-gauche interaction is added between C5 and the methine carbon, C9. While 2 γ-gauche interactions can be tolerable for the C5 carbon, the methine carbon, C9, picks up a third unfavorable γ-gauche interaction with this interchange. This steric problem is resolved by a major change in backbone conformation away form the 3_1 helical conformation.

In Figure 5, one can see qualitatively that the number of γ-gauche interactions is reduced for C9 and C5; however, the existence of non-conventional dihedral angles complicates our interpretation. In essence, one might describe the minimized conformation as a major redirection of the methyl group so that it points away from the helical core; which is the usual status for methyls in the normal 3_1 helix of iPP (Figure 1). This geometrical transformation involves major rotations about the C3-C4, C6-C7 and C7-C9 bonds. In a very crude sense, one might also view the transformation as a moving from the $g^-tg^-tg^-tg^-t$ conformational sequence of the 3_1 helix to a $g^-ttt g^+tg^-t$ sequence in the vicinity of the defect. Note that when the direction of the gauche angle at the site of the defect is reversed (*i.e.*, in the transformation from g^- to g^+), it causes a 120° change in the direction of the stem. The substitution of a trans for a gauche dihedral angle qualitatively compensates for this by rotating the chain 120° in the opposite direction, thereby bringing the rest of the stem back into alignment with the crystal axis.

For this defect conformation, only the downfield shift of methylene carbon, C1, is clearly understood in terms of γ-gauche and vicinal gauche interactions because C1, in the defect structure, has gone from 1 to 0 γ-gauche interactions (C6 is now trans to C1). C6, on the other hand, also has shifted an amount consistent with the loss of a γ-gauche interaction according to the shift calculations. However, we have a harder time rationalizing this since the loss of the γ-gauche interaction with C1 is replaced by a new one with the C2 methyl carbon. In the other direction, the 141° dihedral angle indicates that there are no truly trans or gauche angles and one is left to speculate whether this isn't the most important change influencing the shift of C6. The nature of the dependence of chemical shifts on both γ and vicinal dihedral angles will be explored in a subsequent paper.

In an effort to explore the influence of intermolecular interactions on the chemical shift, quantum mechanical calculations were performed on polymer segments with two nearest-neighbor chains consisting of 5.5 and 3.5 monomers; with the defect in the longer chain. Other researchers have indicated that intermolecular effects are likely to be small in the absence of hydrogen bonding [17,22,23]. Although the results of our calculations are consistent with this hypothesis (in that the maximum effect on the chemical shift of any carbon resulting from the inclusion of the second chain was less than 2 ppm), we found that the small changes in chemical shift brought about by the inclusion of the second chain actually resulted in a noticeable improvement in the agreement between the computed and experimental values. In particular, the relative error of one of the two shifted methylenes is reduced by about 50 % (unfortunately, the error of the other methylene resonance is actually increased) and the position of the deshielded methyl resonance is shifted to a value where it is unambiguously submerged beneath the peak due to the methine carbons in the defect-free polymer. The positions of the other peaks were

essentially uneffected by the inclusion of the second chain. At the present time, it is not clear whether these differences are fortuitous or due a slight, but systematic improvement in the description of the molecular system.

On the basis of the calculations, it appears that each stereo-mrrm defect gives rise to the full set of resonances at 15.9 ppm (methyl-C2), 30.2 ppm (methine-C9), 33.1 ppm (methine-C6), 48.1 ppm (methylene-C4) and 50.5 ppm (methylene-C1); with one peak for each of 5 carbons that are effected by the presence of the defect. This assignment verifies what was previously [2] only an assumption. Hence, the heretofore assumed P_{CR} of 0.48 ± 0.06 for the crystalline partitioning coefficient corresponding to this stereo-mrrm defect [2] is validated. Note that the shift differences, with respect to the main peaks, for this stereo defect that is trapped in a particular conformation, are as much as 6 times larger than the range of shifts covered by stereo-defect-induced variations for corresponding carbons in solution [24]; hence, a knowledge of solution-state shifts for this defect is not very useful for assigning solid-state shifts.

Regio 2,1-erythro Defect

The simulated annealing calculations on this defect were initiated from structures obtained by interchanging the coordinates of a methyl group and a hydrogen on adjacent carbons. Each of the 3 methyl groups at different positions on the helix can, in principle, be exchanged with each of 4 neighboring methylene hydrogens. However, only 6 of these 12 possibilities correspond to erythro isomers; the remaining 6 isomers contain regio 2,1-threo defects. Only the erythro defects are present in the metallocene-synthesized polymers that are considered in this discussion. In contrast to what was observed for both the comonomer and stereo-type defects where the same thermally annealed and energy minimized conformer was obtained from all three initial structures, in the case of the case of the regio 2,1-erythro defect only one out of the six (erythro) placements resulted in a conformer with chemical shifts reasonably consistent with the experimental spectrum. This structure, which holds considerable similarity to the conformer obtained for the stereo-mrrm defect (Figure 5), is displayed in Figure 7. It is, perhaps, understandable that half of the erythro structures do not give good agreement with experiment because, in the normal 3_1 helix of a particular handedness, the backbone-bond directions alternate between a strong and a weak projection onto the helical axis. For a given handedness, there is only one lowest-energy manner in which these bonds alternate. By choosing the direction in which the methyl group is displaced, one dictates the projection on the helical axis of the bond connecting the 2 resulting methine carbons. The steric interactions in these 2 cases are expected to be different; hence, when a thermally annealed and energy minimized conformation is found that relieves each of these steric problems, we might expect that these structures could be very different, both in conformation and in energy. A relevant observation is that one cannot change, e.g. by thermal annealing, the methine-methine bond projection to achieve a more favorable situation for the defect without forcing the entire chain into the higher-energy pattern of bond alternation. Yet, we have a hard time rationalizing why we were only able to generate 1 acceptable conformation out of 6 instead of at least 3 out of 6.

The major difference between this conformation and the one obtained for the stereo defect is that the sequence of 3 trans angles follows, rather than precedes, that unique gauche angle with opposite sign. In addition, unlike what was observed in the case of the stereo defect, where one of the backbone angles was reduced from 180° (in iPP) to 141°, none of the backbone dihedral angles in the structure of the stem containing the regio 2,1-erythro defect are less than 160°. It is not so straightforward to interpret the changes in chemical shifts from a point of view

of γ-gauche or vicinal gauche effects since, with the exception of C8, carbons C4 through C9 are all bonded to or identical to carbons which have changed their identity; hence, their changes in shift will involve influences beyond the γ-gauche or vicinal gauche effects. Nevertheless, we note that methyl carbon C5, the displaced methyl, experiences 3, instead of its usual 1, γ-gauche interactions. Its experimental shift undoubtedly is at 11.9 ppm, i.e. strongly upfield as is expected with that many γ-gauche interactions. Also C6 has 3 γ-gauche interactions instead of the usual 1 for methylene carbons. In addition, methine carbons, C7 and C9, each have only 1, as opposed to their normal 2, γ-gauche interactions. Thus, the γ-gauche interactions will create strong upfield displacements for C5 and C6 and a significant downfield displacement for C7 and C9. In Figure 8, the 3 defect resonances in the 30 ppm to 36 ppm range are all candidates for these C6, C7 and C9 resonances, and we look to the shift calculations to help sort out the assignments.

In the preceding cases, we were able to generate statistics on the computed chemical shifts by considering the values from identical conformations obtained by initiating the simulated annealing process using structures corresponding to the three unique placements of the defect on the 3-monomer repeat unit of the 3_1 helix. In the case of the regio defect, however, this procedure resulted in 3 distinct conformations. Thus, we were forced to adopt a different approach, whereby the simulated annealing calculations were initiated by placing the defect at three *symmetry equivalent* positions on the stem corresponding to 3 different elevations along the crystal axis.

The average chemical shifts and their corresponding uncertainties are presented in Table IV. The chemical shifts for the methylene, methine, and methyl carbons were corrected by Equation 2 for all carbons except C6 and C7. The latter carbons change types between the defective and defect-free chains. It is not clear whether the systematic computational errors are coupled more strongly to chemical functionality or to position in the chain; therefore, for Carbons 6 and C7, we use Equation 3 and Figure 2 to compute shifts.

Those computed values (arrows) which are significantly different from the 3 main iPP shifts are compared to the positions of the experimental defect resonances in Figure 8. The agreement is somewhat less convincing than what was obtained for the other defects because the calculations indicate that there are actually seven, rather than four resonances, which correspond to chemical shifts that *might* be discernible in the experimental spectra of samples containing this defect. Although it is conceivable that 3 of the calculated peaks may be submerged beneath the main resonances, the chemical shifts of at least two carbons (17.3 ppm and 38.6 ppm) are borderline with respect to what we would expect to be able to resolve in the experimental spectrum. In this connection, we note that for all of the defects considered herein, our ability to identify weak resonances near the main peaks is most limited in this sample because of limitations on the available sample concentrations and the smallest P_{CR} value (*vida infra).* Furthermore, as discussed above, the calculated shifts of C6 and C7 are less certain than they are for other carbons. The combined effect of these factors would be expected to result in more significant discrepancies between the computed and experimental spectra than was noted for two previous defects considered.

The relative intensities obtained from integration of the peaks centered at 31.6 ppm, 33.1 ppm, and 35.3 ppm in the experimental spectrum are in the ratio of 1.4:0.5:1.0. Two possible assignments for this resonance pattern were advanced in reference [2]. In the first case, we hypothesized that the feature at 33.1 ppm is the upfield portion of an asymmetric doublet (with the larger downfield portion at 35.3 ppm). Implicit is an assignment of only 2 carbons to these 3 lines with intensities in the ratio of 1.5:1.5 which corresponds to $P_{CR} = 0.32 \pm 0.06$. The other

hypothesis we considered was that the resonance from one carbon belonging to the defect is split, half being at 33.1 ppm and the other half contributing to the resonance at 31.6 ppm. This scenario calls for three carbons with intensities in the ratio of 1:1:1 and gives $P_{CR} = 0.22 \pm 0.04$. Our calculations, which indicate three resonances at 29.9 ppm, 34.9 ppm, and 36.5 ppm corresponding to carbons 6, 7, and 9, would seem to be more consistent with the second postulate. In the final analysis, however, we cannot exclude the possibility that there may be other conformations accepted into the CR that were not identified in our calculations which could also affect the value of P_{CR}. The shape of the methyl resonance in the 10 ppm to 13 ppm range lends credence to the idea that more than one conformer is present. We are hopeful that continued work in this area will lead to a more definitive assignment in the near future.

Butylene Comonomer Defect

Three low-lying conformations were identified in the simulated annealing calculations. In each case, we found that *the backbone conformation remained a 3_1 helix*. The 3 conformations were distinguished by the position of the ethyl-branch methyl (C2) with respect to the backbone methylenes (C1 and C5). The corresponding conformers are referred to in the text as gt, tg, or gg depending on whether C2 (see Figure 9) is, respectively, gauche to C1 and trans to C5, trans to C1 and gauche to C5, or gauche to both C1 and C5. The average chemical shifts, compiled from the results of independent calculations corresponding to 3 different positions of the defect (as described above for both the ethylene comonomer and stereo defects), are listed in Table V. A representative structure (gg), excised from the annealed crystal obtained in one of these simulations, is displayed in Figure 9.

The relative energies obtained from simulated annealing calculations indicate that the gg conformation is the lowest in energy. The corresponding energy of the gt conformation is about 10 kJ/mol higher and the tg another 10 kJ/mol above the gt. As noted previously, we do not give much credence to this aspect of the calculations. In fact, we observed that despite the fact that it had a slightly lower energy than the tg conformation, the gt conformation was unstable during simulated annealing. By this, we mean that, although this structure does correspond to a local minimum in the crystal energy, we observed that it converted to either the tg or gg conformers after a few cycles of simulated annealing. On the other hand, both the gg and tg conformers were found to be stable to annealing in the sense that, once encountered, they would invariably persist to the conclusion of the simulation (50 cycles). Thus, despite the inconsistency in the calculated energies, we believe that only gg and tg conformations are populated to a significant extent in the crystal; with the former being the dominant conformer [4].

The basis of our reasoning is that, when viewed in the context of the calculated values, this appears to be the most reasonable interpretation that is consistent with both the positions and intensities of the observed resonances. The relative intensities obtained by integrating the experimentally observed resonances at 39.5 ppm, 33.0 ppm, 29.7 ppm, 14 ppm, 9 ppm are in the ratio of about 5:1:2:1:2. The last two values represent our best estimates for the centers of, what appears to be, two overlapping methyl peaks extending from about 8 ppm to 16 ppm. The broad shape of this resonance is highly suggestive of the possibility that more than one conformation is populated in the CR. A similar pattern can be obtained from the calculated values (see Table 5 and Figure 10) if it is assumed that only the gg and tg conformers are populated. Thus, ignoring the chemical shifts in Table 5 that belong to the gt conformation and also ignoring those at 44.1 ppm, 27.1 ppm, and 27.7 ppm, which will be submerged beneath the methylene and methine resonances of the defect-free polymer, we obtain 5 lines at approximately 40.6 ppm (averaged

over 3 values), 36.0 ppm, 31.6 ppm, 12.8 ppm, and 7.8 ppm. The empirically determined ratio of 5:1:2:1:2 follows if we assume further that the gg conformer is present at about twice the concentration of the tg conformer. The admission of a third set of resonances from the gt conformer does not seem to result in an equally compelling comparison. The calculated values for the gg and tg conformers are indicated on the experimental spectrum displayed in Figure 10. This assignment is consistent with the value, $P_{CR} = 0.52 \forall 0.08$, that we reported in a previous paper [4].

It is also of interest to note, that the upfield shifts observed for both methylenes (C1 and C5) and the methyl carbon (C2) are consistent with expectations based on the number of γ-gauche interactions. Thus, in the gg conformer both C1 and C5 experience 1 additional γ-gauche interaction (with C2) giving rise to upfield shifts of about 4 ppm for C1 and C5; moreover, C2, the methyl carbon sees a 14 ppm upfield shift with respect to the methyl carbons of iPP. This latter shift is a combination of having 1 additional γ-gauche interaction plus a change from methine to methylene in the type of bonded carbon. For the tg conformer only C5 sees an additional γ-gauche interaction (again with C2) relative to iPP. So again, C5 shifts upfield about 4 ppm. On the other hand, C2 shifts about 9 ppm upfield, even though the number of γ-gauche interactions is the same as for the methyls of CR iPP; therefore, this 9 ppm shift is attributed to the bonding change. A similar analysis has been employed by De Rosa, *et. al.* in interpreting solid state ^{13}C NMR spectra of syndiotactic copolymers of polypropylene and 1-butene [25].

The Influence of Crystal Lattice

In this work we have ignored the issue of the different allomorphs of crystalline iPP, namely, the α- and γ-forms. All of our annealing simulations were done in the α-lattice. The γ-lattice is very unique [26,27] in the sense that the chain axes are not all parallel. Alternating thin layers of parallel chains cross one another at an angle near 80° and all chain axes are inclined at about 40° with respect to the normal to the fold surface. Hence, this lattice is more difficult to model. Usually, for a given molecular mass and a given crystallization history, the ratio of γ- to α-type crystallites increases as the concentration of defects increases. Thus, one might argue that we have not fully explored all possibilities for finding minimum-energy conformations. We cannot deny this. However, in defense of the idea that the low-lying conformations in the α-lattice would look similar to their counterparts in the γ-lattice, we note two things: 1) the energy-minimized conformers in the α-lattice had no intermolecular proton-proton distances which were inordinately short; therefore, the containment potential for the central chain resulting from the surrounding molecules did not seem to place an exceptionally large constraint on any one spot. From this we deduced that minimization of the intramolecular (as opposed to the intermolecular) energetics was also quite important in determining the final conformation. An implication from the latter comment would be that a slight change in the intermolecular potential in going from the α- to the γ-lattice need not lead to a large change in the minimum-energy conformation. 2) Consistent with the foregoing argument, it was also reported [2] that the defect resonances associated with the stereo-mrrm defect did not notably change their chemical shifts for samples that covered the range from fully α to strongly mixed α/γ lattices. It is also worthwhile to note that our conclusions about which conformations are populated in the CR were based partly on a consideration of their relative stability to thermal annealing but more on the agreement between the calculated chemical shifts corresponding to these structures and the observed spectra. We cannot entirely dismiss the possibility that conformations, energy-minimized in the γ-lattice,

would give variants leading to improved fits to the experimental spectra. However, we can reject, on the basis of experimental results, the notion that any of these defects are *restricted* to occupy only those sites belonging to the γ-crystallites.

Summary and Conclusions

A series of defects were introduced at various sites in a molecular model of the α-lattice of crystalline iPP. Low energy conformations were obtained by simulated annealing and the chemical shifts for model stems containing ethylene-comonomer, stereo-mrrm, regio 2,1-erythro, and butylene-comonomer defects were evaluated by performing quantum mechanical calculations on representative segments excised from the annealed and energy-minimized crystallites. The conformational structures of the polymer stems accepted into the crystal region of iPP were inferred by comparing the chemical shifts obtained from these calculations to the experimental patterns of defect resonances. The structures which gave the best agreement with the experimental spectra for each of the four defect types are displayed in Figures 3, 5, 7, and 9. In addition, the resonances in the experimental spectra were assigned to specific carbons. This provided critical support for the crystalline partition coefficients that were advanced on the basis of previous experimental studies and assumptions about defect-resonance assignments. The results of our calculations are consistent with the following values: $P_{CR} = 0.42 \pm 0.03$, $P_{CR} = 0.48 \pm 0.06$, $P_{CR} = 0.22 \pm 0.04$, and $P_{CR} = 0.52 \forall 0.08$, for the ethylene-comonomer, stereo-mrrm, regio 2,1-erythro, and butylene-comonomer defects, respectively.

Acknowledgements

The authors thank Dr. Angel de Dios of Georgetown University for very helpful discussions pertaining to chemical shift calculations. We would also like to acknowledge the efforts of Denis Lehane and Victor McCrary of the High Performance Systems and Services Division at NIST in facilitating access to the computational facilities and software required for the calculations reported in this paper. R.G. Alamo acknowledges support from NSF grant # DMR9753258.

References

1. Fischer, D.; Mülhaupt, R. *Makromol. Chem. Phys*. **1994**, 195, 1433.
2. Vanderhart, D.L.; Alamo, R.G.; Nyden, M.R.; Perez, E.; Mansel, S.; Kim, M-H.; Mandelkern, L. *Macromolecules* **in press**.
3. Alamo, R.G.; Vanderhart, D.L.; Nyden, M.R.; Mandelkern, L. *Macromolecules* **in press**.
4. Vanderhart, D.L. Nyden, M.R., Alamo, R.G., Mandelkern, L. 2000, *ACS PMSE Preprints.*
5. Cheeseman, J.R.; Trucks, G.W.; Keith, T.; Frisch, M.J. *J. Chem. Phys.* **1996**, 104, 5497.
6. Born, R. and Spiess, H.W. In: *NMR Basis Principles and Progress*. Seelig, J., Ed. Springer, Berlin, 1997, 1-125.
7. Vanderhart, D.L.; Pϑrez, E. *Macromolecules* **1986**, 19, 1902.
8. Hikosaka, M.; Seto, T. *Polym. Journal* **1973**, 5, 111.
9. Rutledge, G.C.; Suter, U.W. *Macromolecules* **1992**, 25, 1546.
10. Dauber-Osguthorpe, P.; Roberts, V.A.; Osguthorpe, D.J.; Wolff, J.; Genest, M.; Hagler, A.T. *Function and Genetics* **1988**, 4, 31.

11. Greengard, L.; Rokhlin, V.I. J. Comp. Phys **1987**, 73, 325.
12. Gaussian 98 (Revision A.2), Frisch, M.J.; Trucks, G.W.; Schlegel, H.B.; Scuseria, G.E.; Robb, M.A.; Cheeseman, J.R.; Zakrzewski, V.G.; Montgomery, J.A.; Stratmann, R.E.; Burant, J.C.; Dapprich, S. Millam, J.M.; Daniels, A.D.; Kudin, K.N. Strain, M.C.; Farkas, O.; Tomasi, J.; Barone, V.; Cossi, M.; Cammi, R.; Mennucci, B.; Pomelli, C.; Adamo, C.; Clifford, S.; Ochterski, J.; Petersson, G.A.; Ayala, P.Y.; Cui, Q.; Morokuma, K.; Malick, D.K.; Rabuck, A.D.; Raghavachari, K.; Foresman, J. B.; Cioslowski, J.; Ortiz, J.V.; Stefanov, B.B.; Liu, G.; Liashenko, A.; Piskorz, P.; Komaromi, I.; Gomperts, R.; Martin, R.L.; Fox, D.J.; Keith, T.; Al-Laham, M.A.; Peng, C.Y.; Nanayakkara, A. ; Gonzalez, C.; Challacombe, M.; Gill, P.M.W.; Johnson, B.G.; Chen, W.; Wong, M.W. Andres, J. L.; Head-Gordon, M.; Replogle, E. S. ; Pople, J. A. Gaussian, Inc., Pittsburgh PA (1998).
13. Becke, A.D. *J. Chem. Phys.* **1993**, 98, 5648.
14. Lee, C.; Yang, W.; Parr, R.G., *Phys. Rev. B* **1988**, 37, 785.
15. de Dios, A.C.; Oldfield, E. *J. Am. Chem. Soc.* **1994**, 116, 5307.
16. Harper, J.K.; McGeorge, G. Grant, D.M. *Magn. Reson. Chem.* **1998,** 36, S135
17. Harper, J.K.; McGeorge, G. Grant, D.M. *J. Am. Chem. Soc.* **1999**, 121 6488.
18. Wiberg, K.B. *J. Comp. Chem.* **1999**, 20 1299.
19. Tonelli, A.E., *Macromolecules* **1978**, *11*, 565 and 634. Tonelli, A.E. *NMR Spectroscopy and Polymer Microstructure: The Conformational Connection*, VCH, New York, 1989.
20. Natta, G.; Corradini, P. *Suppl. Nuovo Cimento* **1960**, *15*, 40.
21. Moller, M.; Gronski, W.; Cantow, H.-J.; Hocker, H. *J. Am. Chem. Soc.* **1984**, 106, 5093 5099.
22. Zheng, G.; Wang, L.; Hu, J.; Zhang, X.; Shen, L. Ye, C.; Webb, G.A. *Magn. Reson. Chem.* **1997**, 35, 606.
23. Facelli, J.C.; Pugmire, R.J.; Grant, D.M. *J. Am. Chem. Soc.* **1996**, 118, 5488.
24. Randall, J.C. "*Polymer Sequence Determination: Carbon-13 Method*," Academic Press, New York, **1977**, Chap. 1.
25. De Rosa, C.; Auriemma, F.; Capitani, D.; Caporaso, L.; Talarico, G. *Polymer*, **2000**, 41, 2141.
26. Brückner, S.; Meille, S.V. *Nature* **1989**, *340*, 455.
27. Meille, S.V.;Brückner, S.; Porzio, W. *Macromolecules* **1990**, *23*, 4114.

Table I. Computed and Experimental Chemical Shifts for iPP

Carbon ID	7.5 Monomers[a]	8.5 Monomers[a]
1	48.1 ± 0.03 (3.6)	48.6 ± 0.1 (4.1)
2	22.2± 0.07 (0.1)	22.4 ± 0.02 (0.3)
3	34.6 ± 0.2 (7.9)	32.4 ± 0.5 (5.7)
4	48.2 ± 0.3 (3.7)	49.0 ± 0.2 (4.5)
5	22.1 ± 0.1 (0.0)	22.5 ± 0.2 (0.4)
6	33.8 ± 0.03 (7.1)	33.9 ± 0.2 (7.2)
7	48.4 ± 0.1 (3.9)	48.8 ± 0.08 (4.3)
8	22.1 ± 0.1 (0.0)	22.2 ± 0.2 (0.1)
9	34.4 ± 0.03 (7.7)	33.7 ± 0.1 (7.0)
10	48.4 ± 0.1 (3.9)	49.2 ± 0.2 (4.7)
11	22.1 ± 0.1 (0.0)	22.6 ± 0.2 (0.5)
12	34.2 ± 0.08 (7.5)	34.9 ± 0.3 (8.2)
13	53.3 ± 0.08 (8.8)	49.2 ± 0.2 (4.7)

a. The deviation from the experimental values of 44.5 ppm, 26.7 ppm, and 22.1 ppm, for the methylene, methine, and methyl carbons, respectively are listed in parentheses.

Table II. Computed and Experimental Chemical Shifts for iPP/ETH

Carbon ID	Chemical Shifts		
	Calculated	Corrected	Experimental[a]
1	50.0 ± 0.06	46.4	S
2	22.5 ± 0.4	23.1	S
3	37.0 ± 0.1	29.1	31.1
4	43.5 ± 0.2	39.8	39.2
5	-----	-----	-----
6	30.0 ± 0.2	26.1[b]	24.5[c]
7	38.4 ± 0.5	34.5	34.7
8	21.2 ± 0.3	23.0	S
9	33.6 ± 0.4	25.9	S
10	49.0 ± 0.1	45.1	S
11	22.3 ± 0.2	22.3	S
12	34.8 ± 0.2	27.3	S
13	53.3 ± 0.2	44.5	S

a. The symbol "S" is used when the calculated shift occurs in spectral regions where the methyl, methine, or methylene carbons in iPP resonate so that the peak corresponding to the defective chains is presumed to be submerged beneath a much larger peak due to the defect-free, crystalline iPP carbons.
b. Based on linear correlation summarized in Eq.(3) and Figure 2.
c. Value obtained from polarization/depolarization relaxation experiments.

Table III. Computed and Experimental Chemical Shifts for the stereo-mrrm Defect

Carbon ID	Chemical Shifts		
	Calculated	Corrected[a]	Experimental[b]
1	58.1 ± 0.2	54.0 (52.5)	50.5
2	18.1 ± 0.2	17.8 (17.9)	15.9
3	32.8 ± 0.1	27.1 (25.4)	S
4	53.6 ± 0.1	49.1 (50.2)	48.1
5	22.4 ± 0.1	22.0 (20.5)	S
6	41.0 ± 0.3	33.8 (33.7)	33.1
7	49.2 ± 0.2	44.9 (45.0)	S
8	28.6 ± 0.2	28.5 (26.7)	S
9	37.4 ± 0.4	30.4 (30.0)	30.2
10	49.9 ± 0.3	45.2 (46.2)	S
11	23.1 ± 0.4	22.6 (22.8)	S
12	34.6 ± 0.1	26.4 (28.2)	S
13	48.8 ± 0.1	44.1 (44.1)	S

a. Values in parentheses obtained from quantum mechanical calculations performed on polymer segments containing two, smaller chains (refer to the text for a description of these calculations).

b. The symbol "S" is used when the calculated shift occurs in spectral regions where the methyl, methine, or methylene carbons in iPP resonate so that the peak corresponding to the defective chains is presumed to be submerged beneath a much larger peak due to the defect-free, crystalline iPP carbons.

Table IV. Computed and Experimental Chemical Shifts for the Regio 2,1-erythro Defect

Carbon ID	Chemical Shifts		
	Calculated	Corrected	Experimental[b]
1	52.2 ± 0.08	48.6	S
2	19.7 ± 0.08	19.6	S
3	35.0 ± 0.3	27.1	S
4	42.3 ± 0.1	38.6	S
5	12.1 ± 0.1	12.1	11.9
6	34.4 ± 0.3	29.9[a]	31.6
7	40.0 ± 0.05	34.9[a]	33.1
8	17.3 ± 0.08	17.3	S
9	44.2 ± 0.1	36.5	35.3
10	44.7 ± 0.3	40.8	S
11	22.9 ± 0.1	22.8	S
12	36.3 ± 0.03	28.8	S
13	54.0 ± 0.08	45.2	S

a. Based on linear correlation summarized in Eq.(3) and Figure 2.
b. The symbol "S" is used when the calculated shift occurs in spectral regions where the methyl, methine, or methylene carbons in iPP resonate so that the peak corresponding to the defective chains is presumed to be submerged beneath a much larger peak due to the defect-free, crystalline iPP carbons.

Table V. Computed and Experimental Chemical Shifts for the iPP/BUT Defect

Carbon	Chemical Shifts		
	Calculated	Corrected	Experimental
		gg, tg, gt	
1 (CH_2)	43.9 ± 0.1, 48.0 ± 0.4, 50.2 ± 1.1	40.2[a] ,44.3[a], 46.5[a]	39.5, 44.5
2 $(CH_3)_{eth}$	9.2 ± 0.1, 15.0 ± 0.3, 19.2 ± 0.6	7.8[b], 12.8[b], 16.6[b]	9,14
3 $(CH_2)_{eth}$	31.8 ± 0.4, 31.3 ± 1.0, 39.0 ± 0.4	27.7[b], 27.1[b], 33.9[b]	S
4 $(CH)_{eth}$	36.3 ± 0.1, 41.3 ± 0.3, 41.8 ± 0.8	31.6[b], 36.0[b], 36.4[b]	29.7, 33.0
5 (CH_2)	45.6 ± 0.6, 43.4 ± 1.0, 50.2 ± 0.4	41.9[a],39.7[a], 46.5[a]	39.5

a. Based on Eq.(2) using the values 48.2 ppm and 44.5 ppm for the calculated and experimental chemical shifts of CH_2 carbons in defect-free iPP.

b. Based on linear correlation summarized in Eq.(3) and Figure 2

Figure Captions

1. Model of the α_1 crystallite of iPP consisting of 26 stems of 21-repeat-unit length that was used in the simulated annealing and energy-minimization calculations. The defects were introduced at various positions in the center of the stem indicated by the arrow.

2. Linear correlation between the experimental and computed chemical shifts for iPP, the ethylene comonomer, and stereo-mrrm defects. The slope and intercept obtained from linear regression are 0.879 and –0.304 ppm, respectively.

3. The conformational structure of the ethylene comonomer defect in the α-lattice obtained from the simulated annealing calculations. The values of the backbone dihedral angles are indicated by a number placed above or adjacent to the corresponding bond, depending on whether it is gauche (above) or trans. The labels on the atomic centers correspond to the Carbon ID values listed in Table II.

4. Difference spectrum isolating the resonance-pattern associated with the ethylene comonomer defect. The difference spectrum here, as well as similar 'defect' spectra in Figures 6, 8 and 10, is generated from spectra of crystalline regions only. These difference spectra, to first order, are corrected by spectral subtraction (see text) for the presence of known amounts of other types of defects whose resonances we wish to suppress. (It is difficult to find samples with just a single type of defect.) The arrows indicate the values of the corrected chemical shifts obtained from the calculations. The off-scale peaks at 44.5 ppm, 26.7 ppm and 22.1 ppm correspond to the methylene, methine and methyl resonances in iPP; however, owing to the spectral subtractions, the intensity ratios between these large iPP resonances and the defect resonances lose their significance. At the same time, the relative intensities among the defect peaks retain their significance. The tiny shoulder at 24.5 ppm is due to the resonance of carbon 6 in iPP/ETH.

5. The conformational structure of a stem containing a stereo-mrrm defect obtained from the simulated annealing calculations. The values of the backbone dihedral angles are indicated by a number placed above or adjacent to the corresponding bond. The labels on the atomic centers correspond to the Carbon ID values listed in Table III.

6. Difference spectrum isolating the resonance-pattern associated with the stereo-mrrm defect. The arrows indicate the values of the corrected chemical shifts obtained from the calculations. See the caption of Figure 4 for other details.

7. The conformational structure of a stem containing a regio 2,1-erythro defect obtained from the simulated annealing calculations. The values of the backbone dihedral angles are indicated by a number placed above or adjacent to the corresponding bond. The labels on the atomic centers correspond to the Carbon ID values listed in Table IV.

8. Difference spectrum isolating the resonance-pattern associated with the 2,1-erythro defect. The arrows indicate the values of the corrected chemical shifts obtained from the calculations. See the caption of Figure 4 for other details.

9. The conformational structure of a stem containing a butylene comonomer defect obtained from the simulated annealing calculations. Three conformers were identified. Only the gg (see text for defintion) is displayed here. The labels on the atomic centers correspond to the Carbon ID values listed in Table V.

10. Difference spectrum isolating the resonance-pattern associated with the butylene comonomer defect. The values of the corrected chemical shifts are indicated by arrows with and without filled circles corresponding to the tg and gg conformers, respectively. In the process of subtracting the contributions from the regio 2,1 erythro defects and the mrrm-stereo defect, most of the intensity of the main iPP resonances is lost. This allows one to identify the resonances associated with the butylene defect more easily. At the same time, one must not confuse the large fluctuations in the immediate vicinity of the main resonances with defect resonances. These fluctuations arise because the detailed shapes of the parent resonances vary slightly from sample to sample.

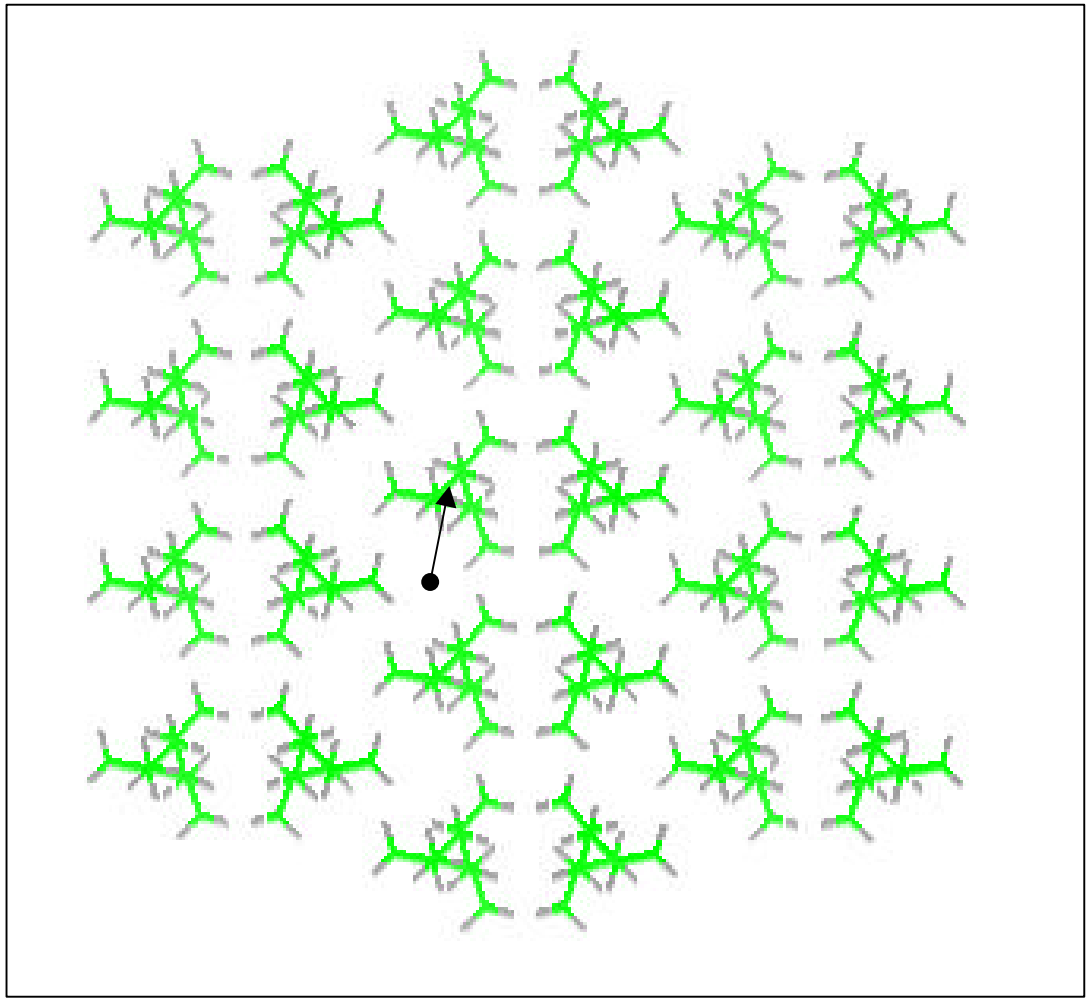

Figure 1

Experimental vs Computed Chemical Shifts

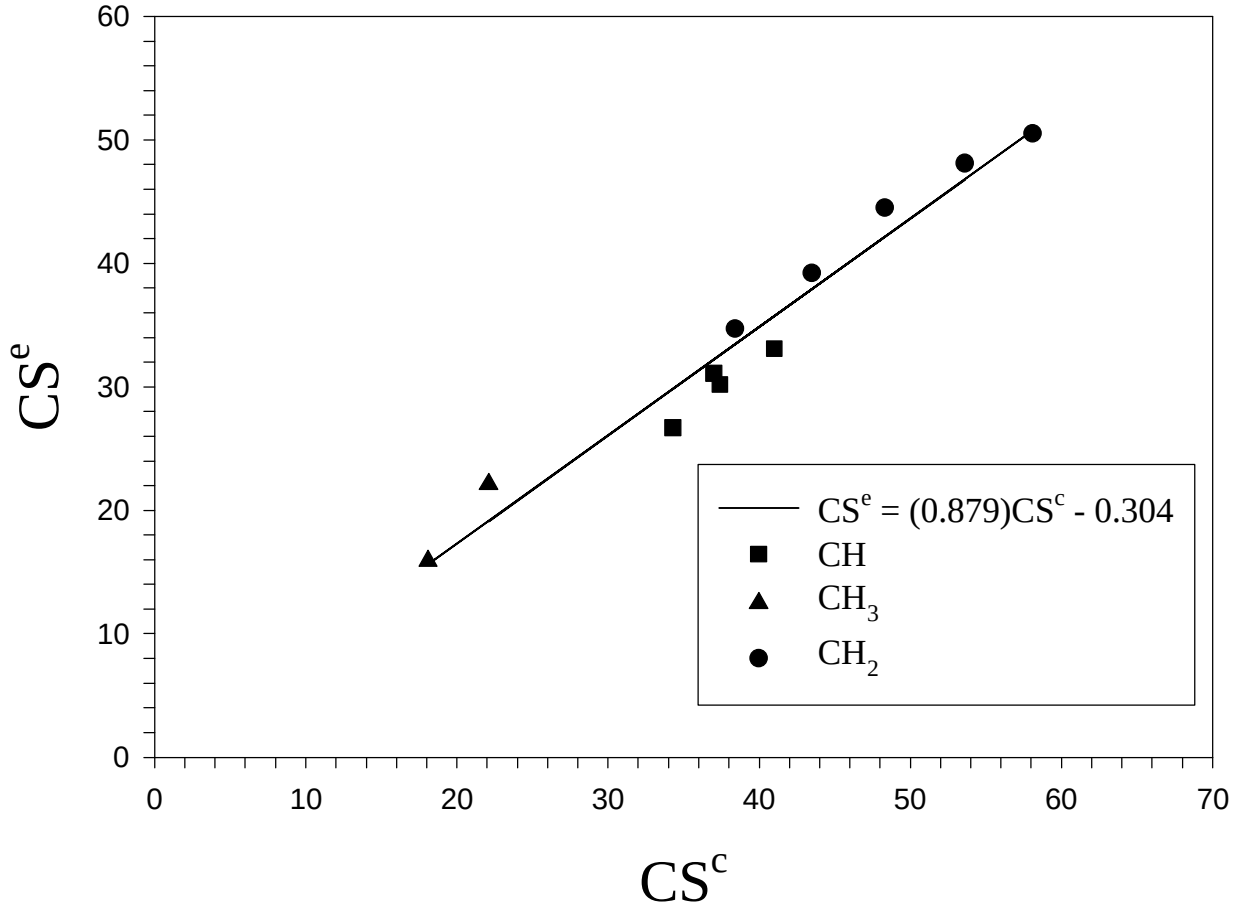

Figure 2

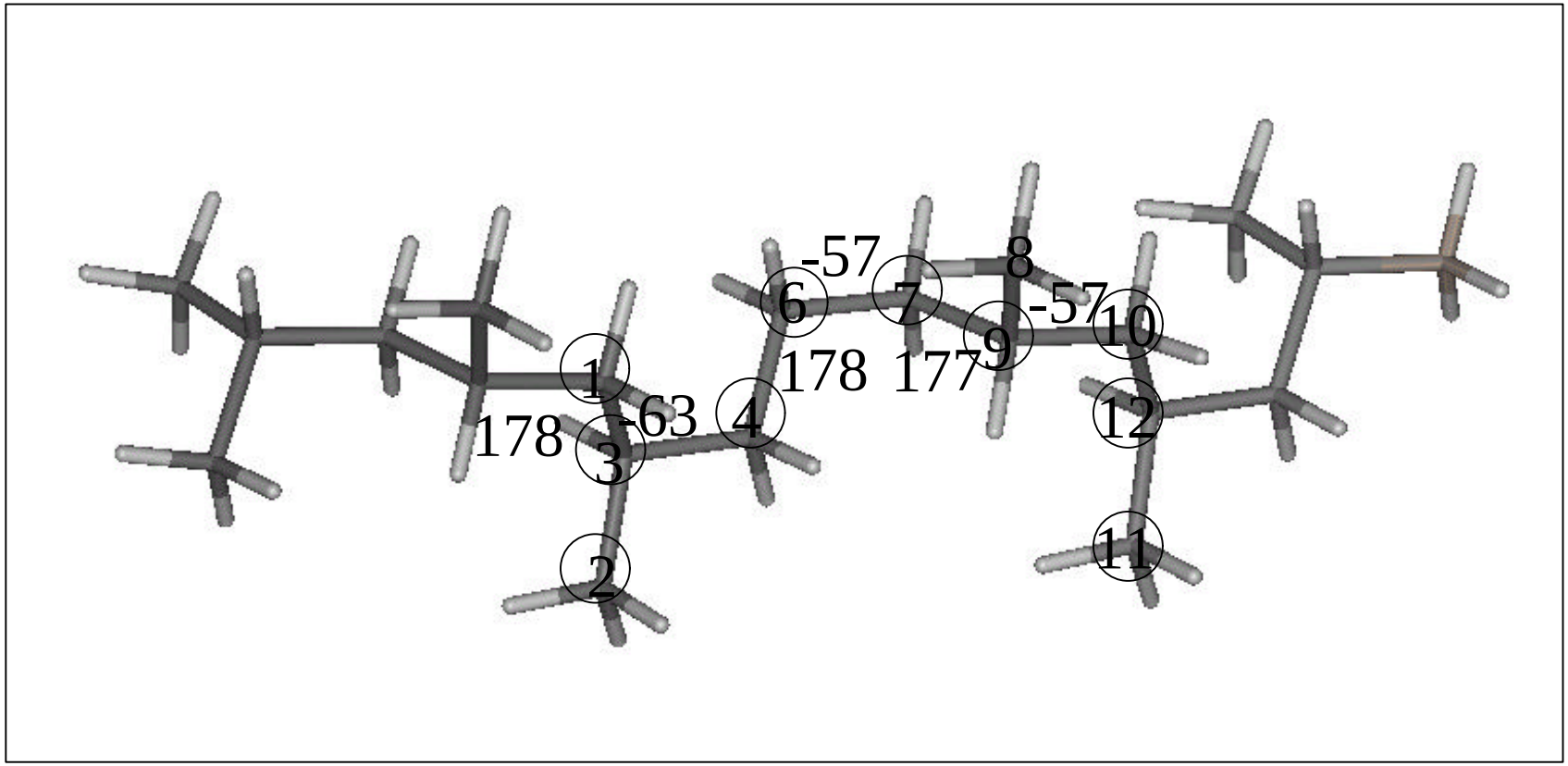

Figure 3

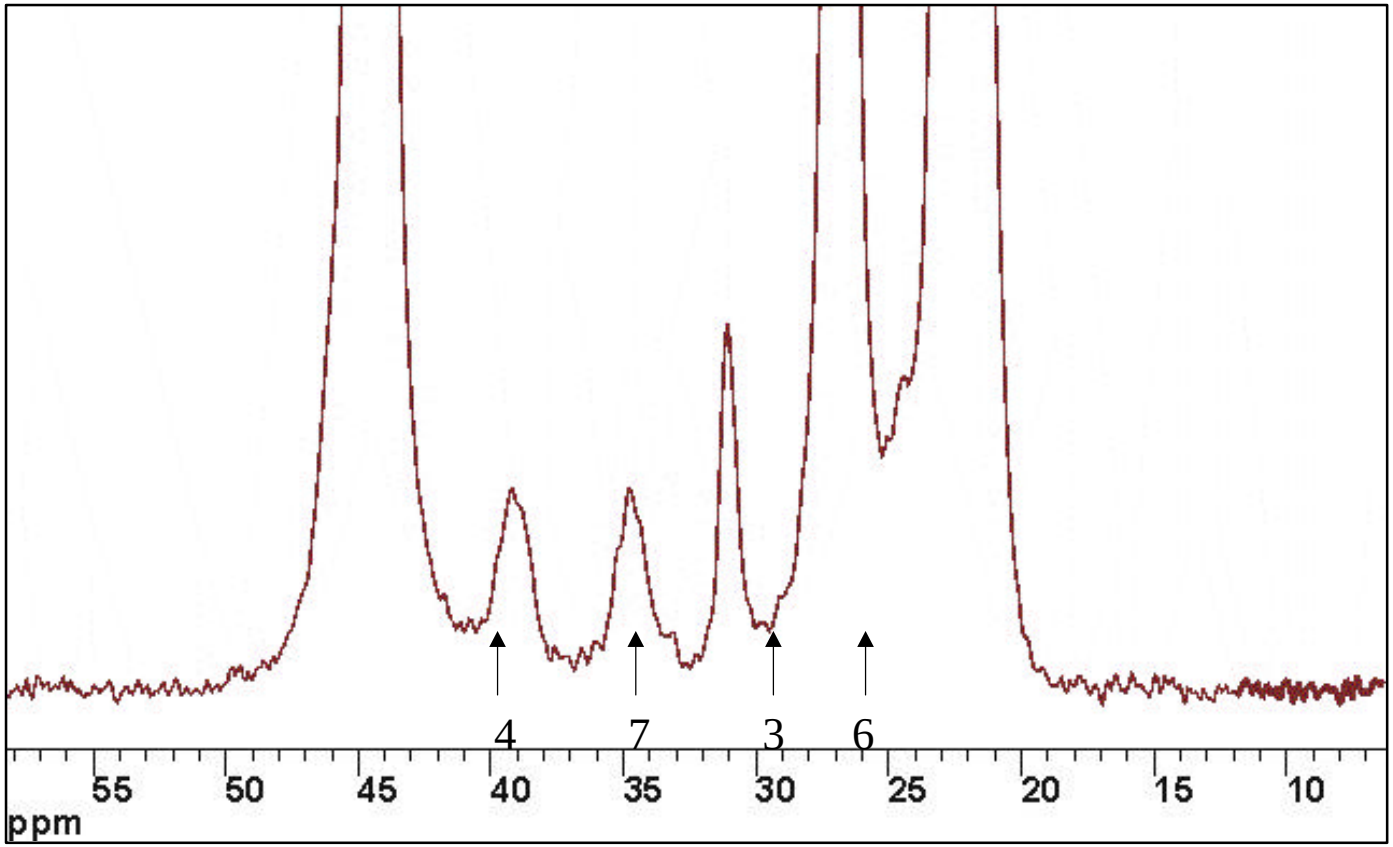

Figure 4

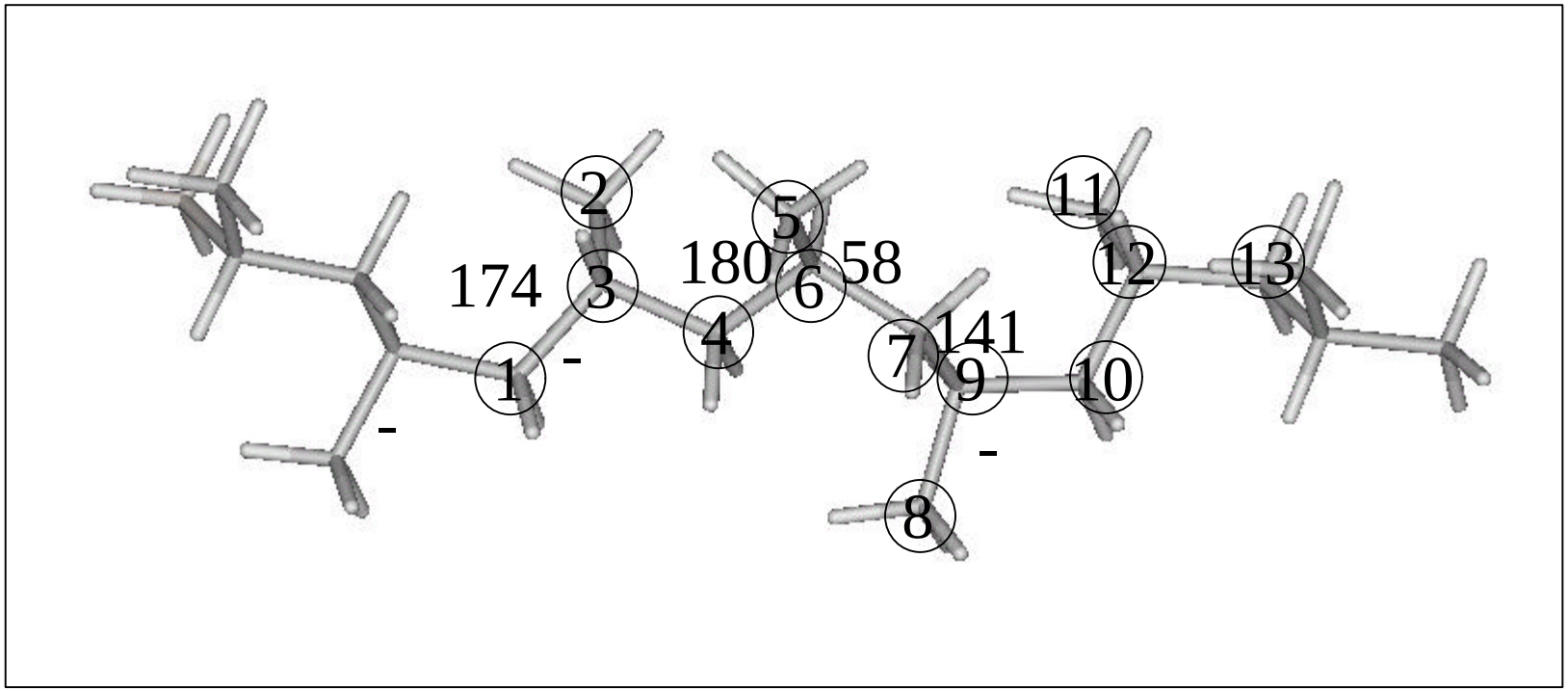

Figure 5

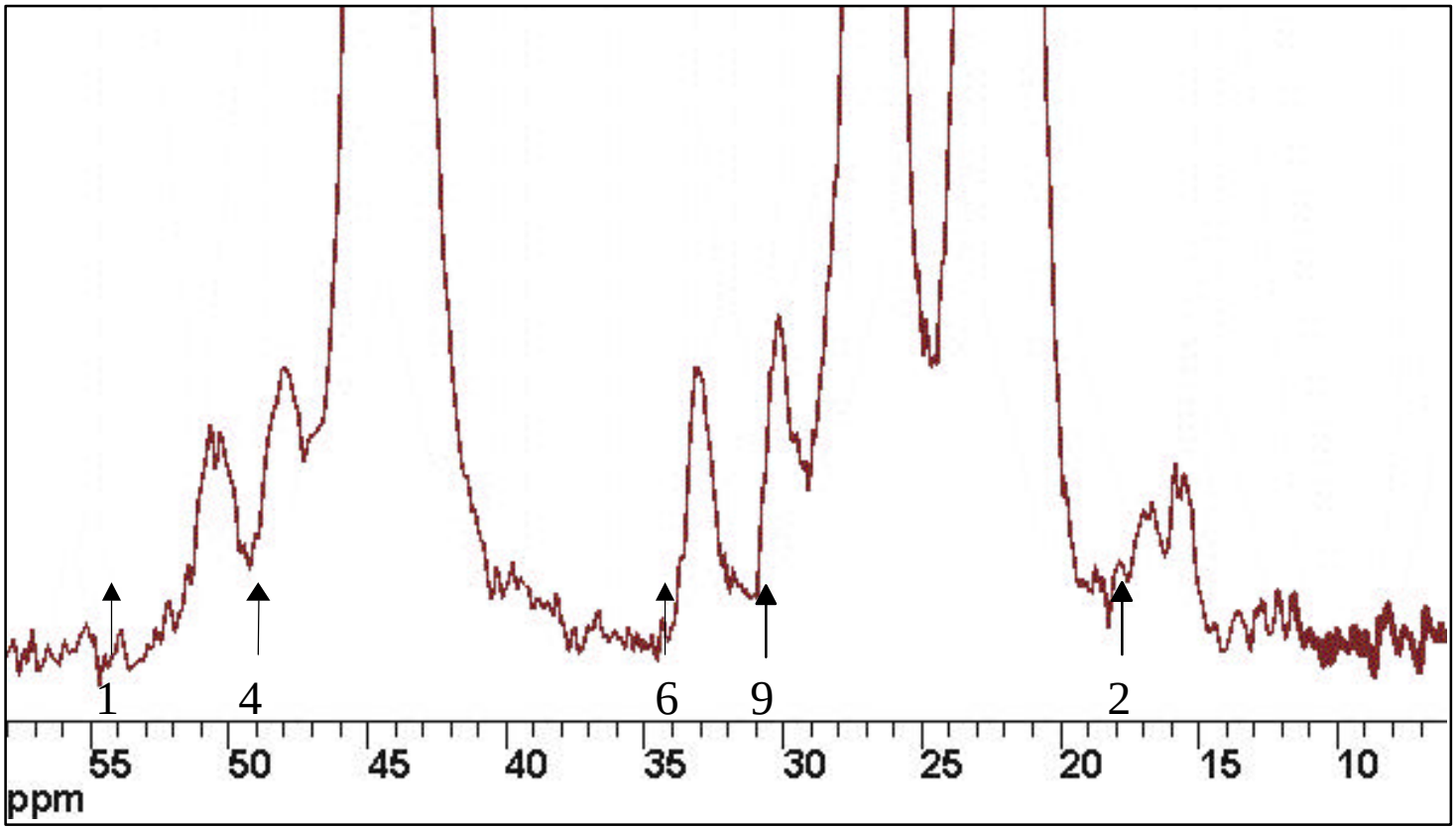

Figure 6

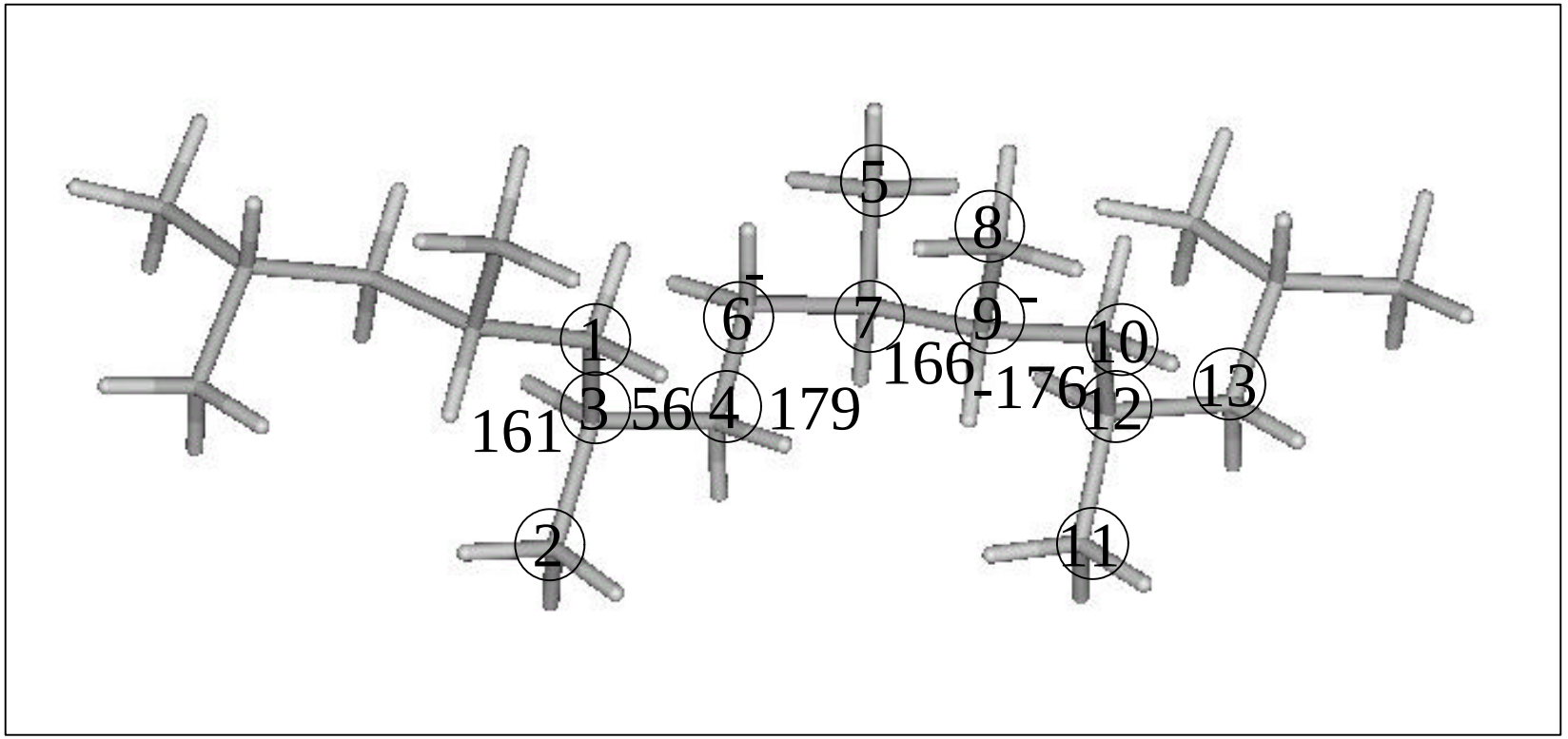

Figure 7

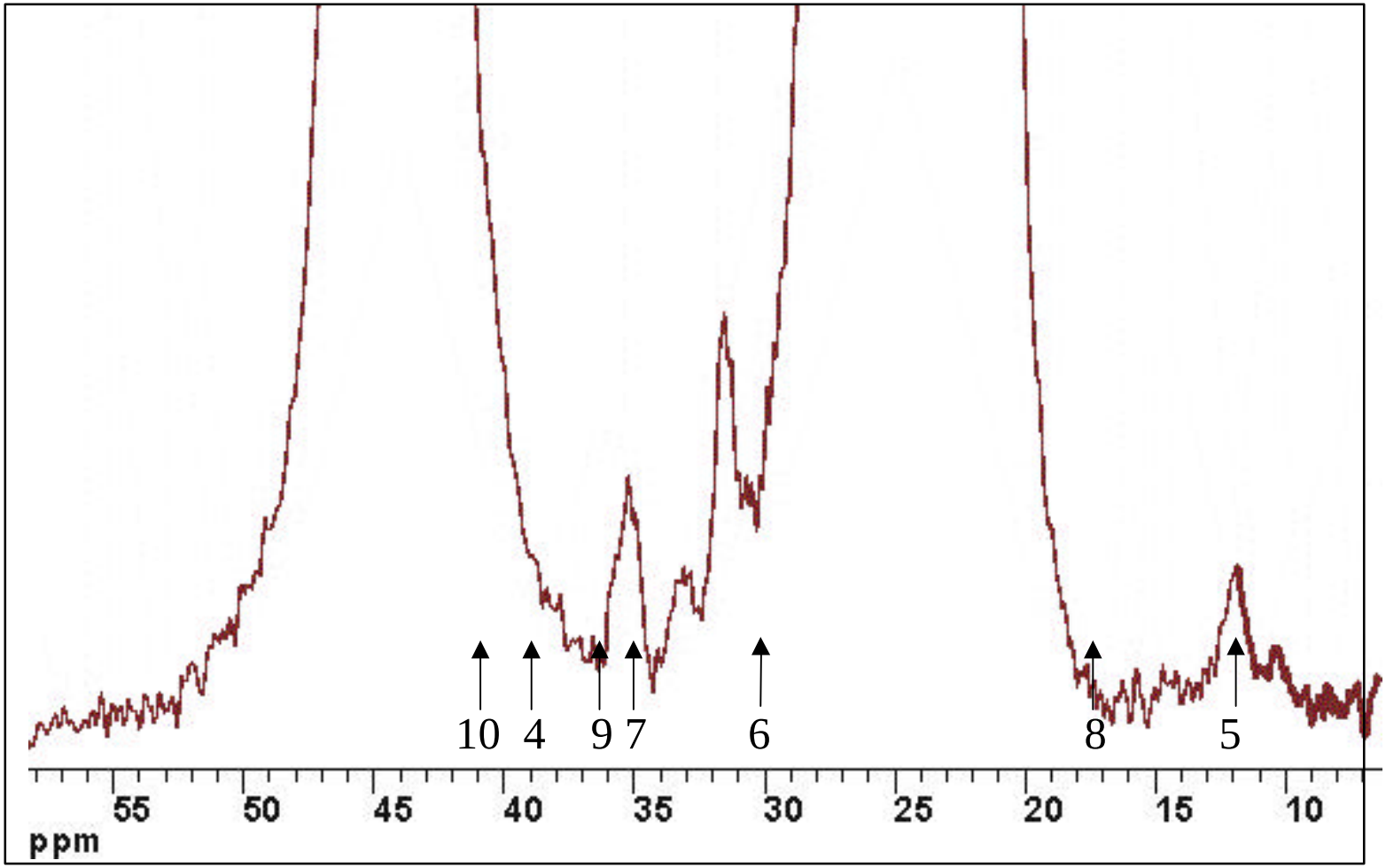

Figure 8

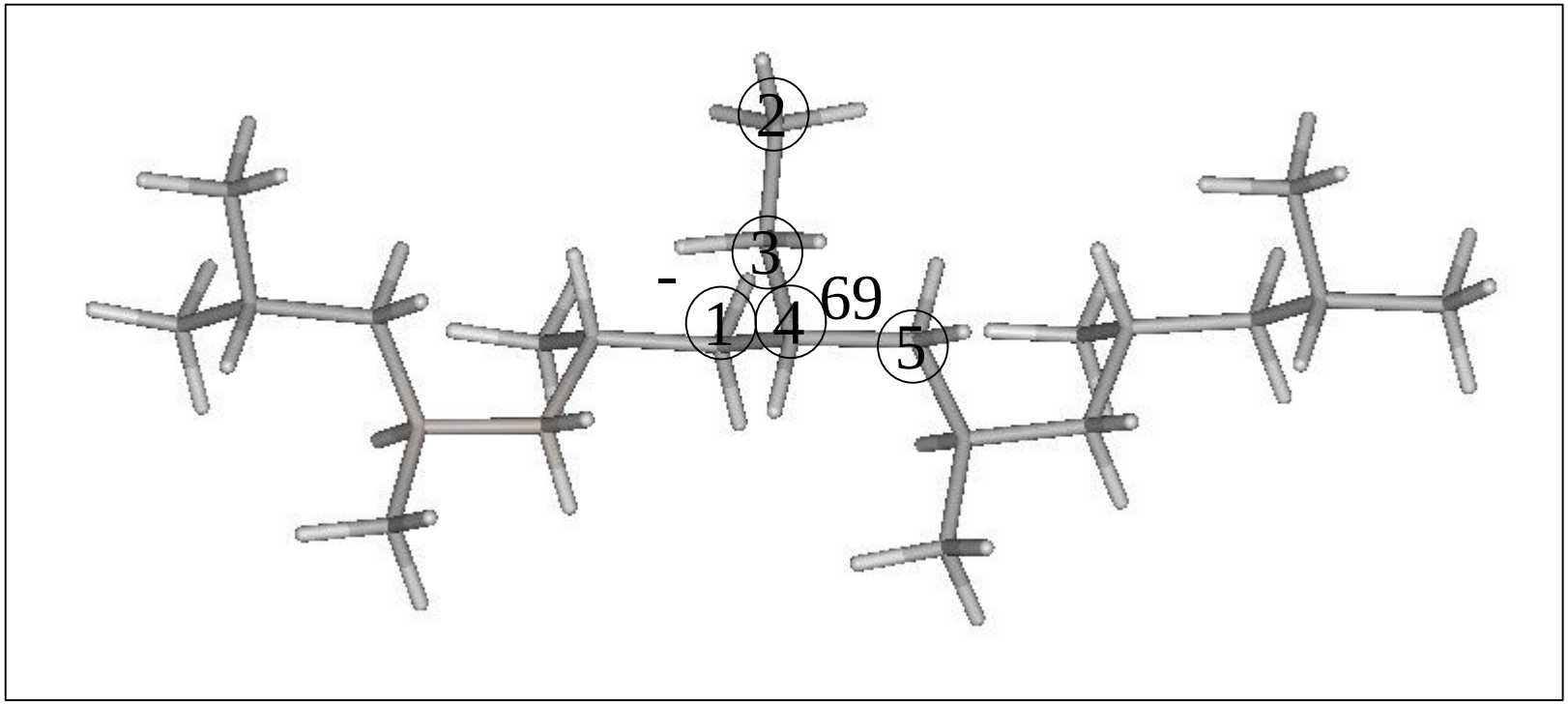

Figure 9

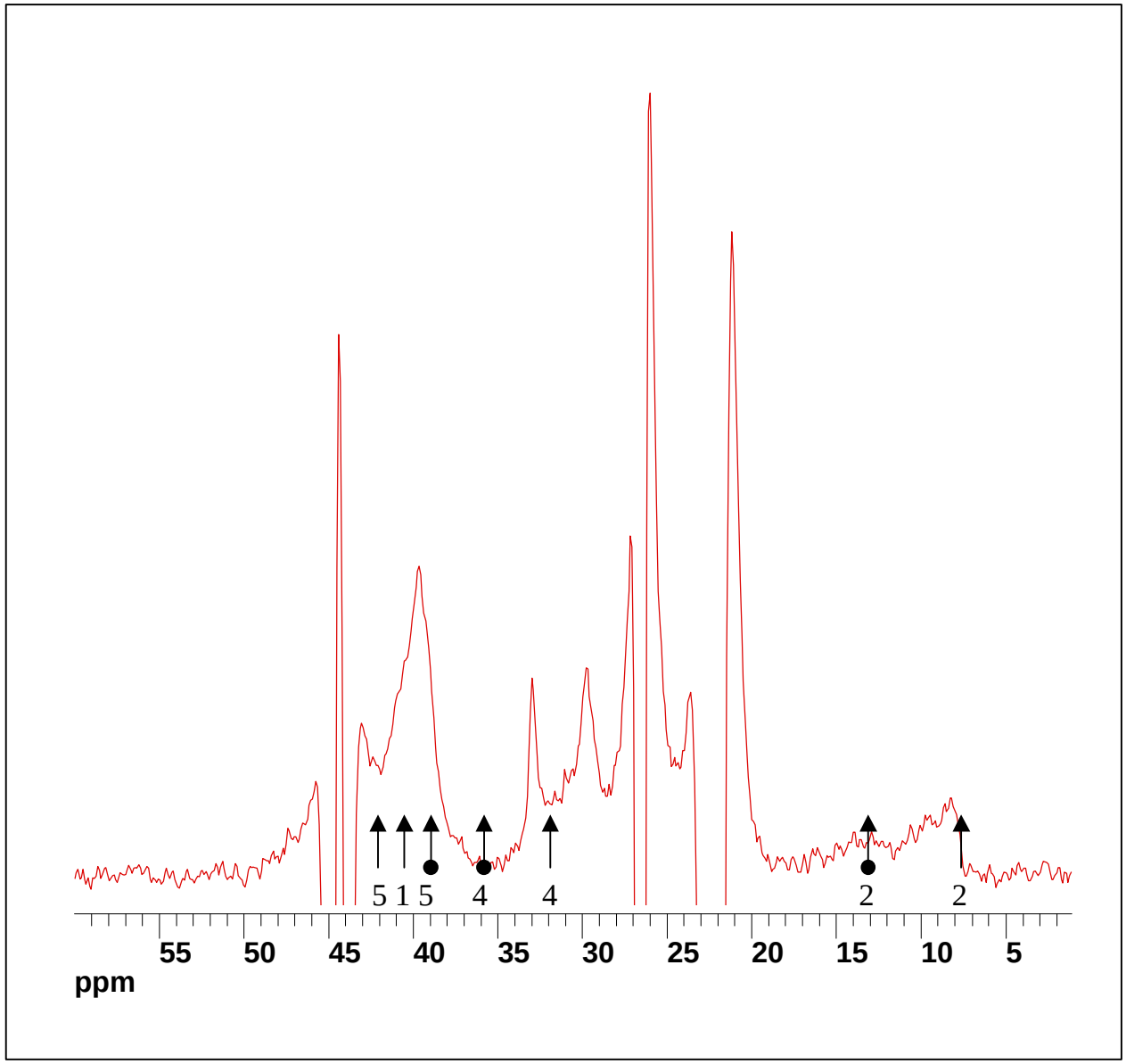

Figure 10